

Back to MLP: A Simple Baseline for Human Motion Prediction

Wen Guo*, Yuming Du*†, Xi Shen†, Vincent Lepetit, Xavier Alameda-Pineda, and Francesc Moreno-Noguer

Abstract—This paper tackles the problem of human motion prediction, consisting in forecasting future body poses from historically observed sequences. Despite of their performance, current state-of-the-art approaches rely on deep learning architectures of arbitrary complexity, such as Recurrent Neural Networks (RNN), Transformers or Graph Convolutional Networks (GCN), typically requiring multiple training stages and more than 3 million of parameters. In this paper we show that the performance of these approaches can be surpassed by a light-weight and purely MLP architecture with only 0.14M parameters when appropriately combined with several standard practices such as representing the body pose with Discrete Cosine Transform (DCT), predicting residual displacement of joints and optimizing velocity as an auxiliary loss.

An exhaustive evaluation on Human3.6M, AMASS and 3DPW datasets shows that our method, which we dub siMLPe, consistently outperforms all other approaches. We hope that our simple method could serve a strong baseline to the community and allow re-thinking the problem of human motion prediction and whether current benchmarks do really need intricate architectural designs. Our code is available at <https://github.com/dulucas/siMLPe>.

Index Terms—Human Motion Prediction, MLP, Simple Baseline.

arXiv:2207.01567v1 [cs.CV] 4 Jul 2022

1 INTRODUCTION

Given a sequence of 3D human poses, the task of human motion prediction aims to predict the follow-up of the pose sequence. Forecasting future human motion is of vital importance, and potential applications include preventing accidents in autonomous driving [1], tracking people [2], or interacting with a robot [3]

Due to the spatio-temporal nature of the human motion signal, the common trend in the literature is to design models enable capture spatial and temporal information. Traditional approaches mainly rely on hidden Markov models [4] or Gaussian process latent variable models [5]. Although they perform well on simple and periodic motion patterns, they fail dramatically when encountering complex motions [6]. Recently, with the success of deep learning and neural networks, various methods have been developed based on different types of neural networks that are able to handle sequential data, including Recurrent Neural Networks (RNN) [7], Graph Convolutional Networks (GCN) [6] and Transformers [8]. However, these architectures are often

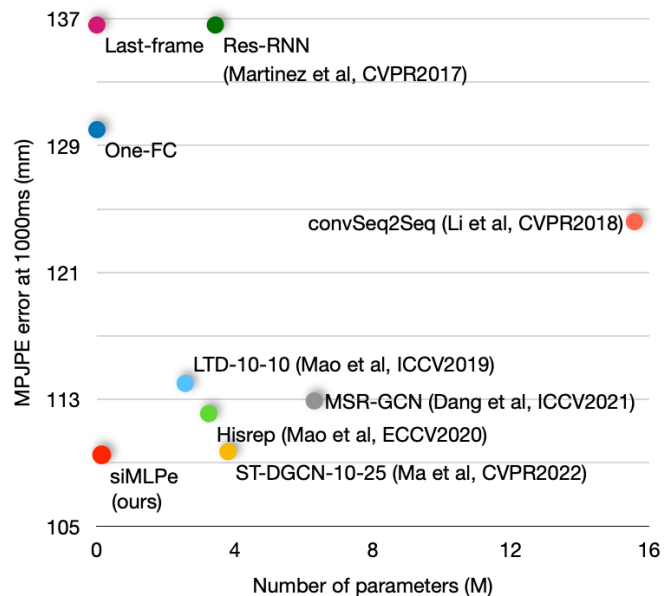


Fig. 1. Comparison of parameter size and performance on Human3.6M dataset [9]. we report MPJPE in *mm* at 1000 ms. Our method can achieve the lowest error with significantly less parameters. 25]. We also show performances of two simple baselines: 'Last Frame' takes the last input frame as output, 'One FC' uses only one single fully connected layer. These two naive methods could already achieve comparable results than some classical approaches.

complex and exploit the aforementioned components to fuse the information across human joints and time.

In this paper, we propose siMLPe, a simple yet effective network, which is merely composed of multi layer perceptrons (MLPs) but able to encode the variability of human motion. Specifically, our proposed network is illustrated in

- * Equal contribution.
- † Corresponding author.
- W. Guo, X. Alameda-Pineda are with INRIA Grenoble Rhône-Alpes and Université Grenoble Alpes, France. Wen is also with Institut de Robòtica i Informàtica Industrial (CSIC-UPC), Barcelona, 08028, Spain. Email: {wen.guo,xavier.alameda-pineda}@inria.fr.
- Y. Du, V. Lepetit are with LIGM, Ecole des Ponts, Univ Gustave Eiffel, CNRS, Marne-la-vallee, France. Email: {yuming.du, vincent.lepetit}@enpc.fr.
- X. Shen is with Tencent AI Lab, Shenzhen, China. Email: tison-shen@tencent.com.
- F. Moreno-Noguer is with Institut de Robòtica i Informàtica Industrial (CSIC-UPC), Barcelona, 08028, Spain. E-mail: fmoreno@iri.upc.edu.

Figure 2 and composed of a series of fully connected layers, layer normalization [10] and spatial-temporal transpose operation. Even the commonly used activation layers such as ReLU [11] are not necessary. Despite its simplicity, siMLPE is able to achieve strong performance when appropriately combined with standard practices, such as representing the body pose with Discrete Cosine Transform (DCT), predicting residual displacement of joints and optimizing velocity as an auxiliary loss.

Precisely, our approach siMLPE obtains state-of-the-art performance on several standard benchmarks including Human3.6M [9], AMASS [12] and 3DPW [13]. siMLPE is also light-weight and contains $20\times$ to $60\times$ less parameters than competitive approaches. Figure 1 shows the comparison of Mean Per Joint Position Error (MPJPE) at 1 000ms on Human3.6M [9] as well as the number of parameters used in each approach, which demonstrates the effectiveness and efficiency of our approach.

Interestingly, in extreme cases, leveraging the pose from the last frame (‘Last-frame’) achieves long-term prediction close to Res-RNN [7] and using a single FC layer (‘One-FC’) allows obtaining even better performance than Res-RNN [7]. Note that Res-RNN [7] is a much more complex model based on RNN. These observations suggest as a sequential prediction task, human motion prediction can be tackled in a completely different way using directly simple MLP. We expect our method could serve as a baseline for the future research and help the community to rethink the task of human motion prediction. Our implementation is available at <https://github.com/dulucas/siMLPE>.

In summary, our contributions are as follows:

- We propose siMLPE, a simple yet effective baseline with only MLP layers for human motion prediction, achieving state-of-the-art performance with far less parameters than existing methods on multiple benchmarks like Human3.6M [9], AMASS [12] and 3DPW [13] datasets.
- We show that the human motion prediction can be modelled in a simple way without explicitly fusing spatial and temporal information. As an extreme example, a single FC layer can already achieve good performance.

2 RELATED WORK

Human motion prediction is formulated as a sequence-to-sequence task, where past observed motion is taken as input to predict the future motion sequence. Traditional methods explore human motion prediction with nonlinear Markov models [14], Gaussian Process dynamical models [15], and Restricted Boltzmann Machine [16]. These approaches have shown to be effective to predict simple motions and eventually struggle on complex and long-term motion prediction [17]. In deep era, human motion prediction has achieved great success with the use of deep networks, including Recurrent Neural Network(RNN) [7, 17–20], Graph Convolutional Network(GCN) [6, 21–26] and Transformer [8], which are the main focus of this section.

2.1 RNN-based human motion prediction

Due to the inherent sequential structure of human motion, 3D human motion prediction has been mostly addressed with recurrent models. Fragkiadaki *et al.* [17] propose an encoder-decoder framework to embed human poses and an LSTM to update the latent space and predict future motion. Jain *et al.* [18] manually encodes the semantic similarity between different parts of the body and forwards them via structural RNNs. However, these two methods suffer from discontinuity and they only trained action-specific models, *i.e.* a single model is trained for a specific action.

Martinez *et al.* [7] studied multi-actions instead of action-specific models *i.e.* train one single model for multiple actions, which is in practice more interesting and allows the network to exploit regularities across different actions in large scale datasets. This is widely adopted by most of the motion works until now. They also introduced a residual connection to model the velocities instead of the absolute value to have more smooth predictions.

The above-mentioned methods also suffer from multi-inherent disadvantages of RNN. First, as a sequential model, RNN is difficult for parallelization during training and inference. Second, the memory constraints prevent RNN from exploring information from farther frames. Some works alleviate this problem by using RNN variants [19, 20], sliding windows [27, 28], convolutional models [29, 30] or adversarial training [31].

2.2 GCN-based human motion prediction

To better encode the spatial connectivity of human joints, the most recent works usually build the human pose as a graph and adopt Graph Convolutional Networks(GCNs) [32, 33] for human motion prediction.

GCNs are first adopted in human motion prediction in Mao *et al.* [6]. They use a stack of blocks consisting of GCNs, non linear activation and batch normalization to encode the spatial dependencies, and leverage discrete cosine transform (DCT) to encode temporal information. This work inspired most of the GCN-based motion prediction methods in recent years. Based on [6], Mao *et al.* [21] further improved the temporal encoding by cutting the past observations into several sub-sequences, and adding an attention mechanism to find similar previous motion sub-sequences in the past with the current observations. Thus the future sequence is computed as a weighted sum of observed sub-sequences. Then a GCN based predictor, exactly the same as that of Mao *et al.* [6], is used to encode the spatial dependencies. Instead of using DCT to encode the input sequence, [34] used a multi-scale temporal input embedding, by applying various size convolutional for different input sizes to have different receptive fields in the temporal domain. Ma *et al.* [23] proposes two variants of GCN to extract spatial and temporal features. They build a multi-stage structure where each stage contains an encoder and a decoder, and during the training, the model is trained with intermediate supervision to learn to progressively refine the prediction. Besides, [24–26] extend the graph of human pose to multi-scale version across the abstraction levels of human pose.

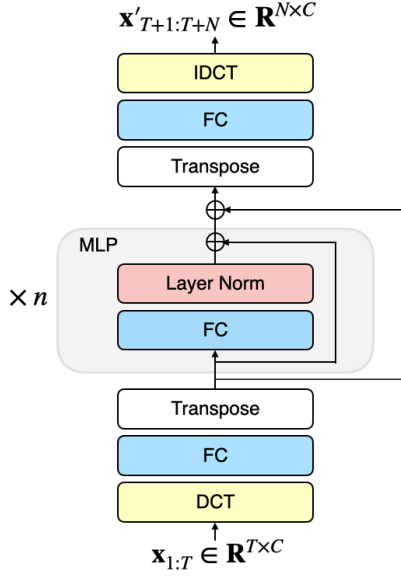


Fig. 2. Overview of our approach siMLPE for human motion prediction. FC denotes a fully connected layer, Layer Norm denotes a layer normalization [10] operation. DCT and IDCT represent the discrete cosine transformation and inverse discrete cosine transformations respectively. The MLP blocks in gray (composed of FC and Layer Norm) are repeated n times.

2.3 Attention-based human motion prediction

With the development of transformer [35], some works [8, 21, 36] tried to deal with this task with attention mechanism. Beside of [21] which adopted attention to find temporal relations, [8] use attentions to map not only the temporal dependencies but also the pairwise relation of joints by an architecture which combines spatial-attention and temporal-attention in parallel. Moreover, [36] used a transformer-based architecture along with a progressive-decoding strategy to predict the DCT coefficients of the target joints progressively based on the kinematic tree. In order to guide the predictions, they also built a memory-based dictionary to preserve the global motion patterns in training data.

With the development of human motion prediction in recent years, the RNN/GCN/transformer based architectures are well explored and the results have been significantly improved. Though these methods are shown to be effective, the architectures are becoming more and more complicated and difficult to train. In this paper, we stick to simple architectures and propose a MLP-based network. We hope that our simple method would serve a baseline and let the community rethink the problem of human motion prediction.

3 OUR APPROACH : siMLPE

Given a sequence of 3D human poses in the past, our goal is to predict the future 3D human poses. Our approach is illustrated in Figure 2. We first present how to pre-process motion data in Section 3.1. The components of the network are detailed in Section 3.2. In Section 3.3, we detail the losses we use for training.

We denote the observed 3D human poses as $\mathbf{x}_{1:T} = [x_1^\top, \dots, x_T^\top]^\top \in \mathbf{R}^{T \times C}$, consisting of T consecutive hu-

man poses, where the pose at the t -th frame x_t is represented by a C -dimensional feature, i.e. $x_t \in \mathbf{R}^C$. Our goal is to predict the future N motion frames $\mathbf{x}_{T+1:T+N} = [x_{T+1}^\top, \dots, x_{T+N}^\top]^\top \in \mathbf{R}^{N \times C}$. In this work, we follow previous works [6, 7, 21, 23] and adopt the 3D coordinates of the joints as our motion representation.

3.1 Discrete Cosine Transform (DCT)

We use the Discrete Cosine Transform (DCT) to encode temporal information, which is proven to be beneficial for human motion prediction [6, 21, 23]. More precisely, given an input motion sequence of T frames, the DCT matrix $\mathbf{D} \in \mathbf{R}^{T \times T}$ can be calculated as:

$$\mathbf{D}_{i,j} = \sqrt{\frac{2}{T}} \frac{1}{\sqrt{1 + \delta_{i,0}}} \cos\left(\frac{\pi}{2T}(2j+1)i\right), \quad (1)$$

where $\delta_{i,j}$ denotes the Kronecker delta function:

$$\delta_{i,j} = \begin{cases} 1 & \text{if } i = j \\ 0 & \text{if } i \neq j. \end{cases} \quad (2)$$

The transformed input is $\mathcal{D}(\mathbf{x}_{1:T}) = \mathbf{D}\mathbf{x}_{1:T}$. For the output, we apply the Inverse Discrete Cosine Transform (IDCT) to transform the output of the network to the original pose representation, denoted as \mathcal{D}^{-1} and the inverse of \mathbf{D} .

3.2 Network Architecture

The architecture of our network is shown in Figure 2. Our network only contains three components, the fully connected layers, the transpose operation and layer normalization [10]. For the all the fully connected layers, their input dimension is equal to their output dimension. In this paper, we call a block containing one fully connected layer and one layer normalization [10] with skip connection a MLP block, as shown in the Figure 2. After the DCT transformation, a motion sequence is first fed to a fully connected layer and a transpose layer, then the output feature is fed to n consecutive MLP blocks. In the end, the extracted feature is transposed back to the original dimension and fed to a fully connected layer, the predicted motion is obtained by applying the IDCT to the output of the last fully connected layer.

3.3 Losses

In practice, instead of predicting the absolute coordinates of joints in each frame, we predict the difference between the future frames and the last frame of the input motion sequence. Therefore, the output of the network is actually $x_{T+t} - x_T$.

Objective function. Our objective function \mathcal{L} includes two terms \mathcal{L}_{re} and \mathcal{L}_v ,

$$\mathcal{L} = \mathcal{L}_{re} + \mathcal{L}_v. \quad (3)$$

\mathcal{L}_{re} aims at minimizing the L2-norm between the predicted motion $\mathbf{x}'_{T+1:T+N}$ and ground-truth one $\mathbf{x}_{T+1:T+N}$:

$$\mathcal{L}_{re} = \mathcal{L}_2(\mathbf{x}'_{T+1:T+N}, \mathbf{x}_{T+1:T+N}). \quad (4)$$

TABLE 1

Results on Human3.6M [9]. We report MPJPE error in *mm*. † indicates that the result is taken from Hisrep [21], * indicated that the result is taken from ST-DGCN [23]. We also show results of two simple baselines: 'Last Frame' takes the last input frame as output, 'One FC' uses only one single fully connected layer. These two implementations could already achieve comparable results with early methods like [7].

| Time (ms) | MPJPE (mm) ↓ | | | | | | | | # Param.(M) ↓ |
|----------------------|--------------|-------------|-------------|-------------|-------------|-------------|--------------|--------------|---------------|
| | 80 | 160 | 320 | 400 | 560 | 720 | 880 | 1000 | |
| Last Frame | 23.8 | 44.4 | 76.1 | 88.2 | 107.4 | 121.6 | 131.6 | 136.6 | 0 |
| One FC | 14.0 | 33.2 | 68.0 | 81.5 | 101.7 | 115.1 | 124.8 | 130.0 | 0.003 |
| Res-RNN † [7] | 25.0 | 46.2 | 77.0 | 88.3 | 106.3 | 119.4 | 130.0 | 136.6 | 3.44 |
| convSeq2Seq † [30] | 16.6 | 33.3 | 61.4 | 72.7 | 90.7 | 104.7 | 116.7 | 124.2 | 15.58 |
| LTD-10-10 † [6] | 11.2 | 23.4 | 47.9 | 58.9 | 78.3 | 93.3 | 106.0 | 114.0 | 2.56 |
| Hisrep † [21] | 10.4 | 22.6 | 47.1 | 58.3 | 77.3 | 91.8 | 104.1 | 112.1 | 3.24 |
| MSR-GCN * [24] | 11.3 | 24.3 | 50.8 | 61.9 | 80.0 | - | - | 112.9 | 6.30 |
| ST-DGCN-10-25 * [23] | 10.6 | 23.1 | 47.1 | 57.9 | 76.3 | 90.7 | 102.4 | 109.7 | 3.80 |
| siMLPE(Ours) | 9.6 | 21.9 | 46.5 | 57.5 | 75.8 | 90.1 | 101.8 | 109.5 | 0.14 |

TABLE 2

Results on AMASS-BMLrub [12] and 3DPW [13]. We report MPJPE error in *mm*. The model is trained on AMASS dataset. State-of-the-art results are taken from Hisrep [21].

| Time (ms) | AMASS | | | | | | | | 3DPW | | | | | | | |
|------------------|-------------|-------------|-------------|-------------|-------------|-------------|-------------|-------------|-------------|-------------|-------------|-------------|-------------|-------------|-------------|-------------|
| | 80 | 160 | 320 | 400 | 560 | 720 | 880 | 1000 | 80 | 160 | 320 | 400 | 560 | 720 | 880 | 1000 |
| convSeq2Seq [30] | 20.6 | 36.9 | 59.7 | 67.6 | 79.0 | 87.0 | 91.5 | 93.5 | 18.8 | 32.9 | 52.0 | 58.8 | 69.4 | 77.0 | 83.6 | 87.8 |
| LTD-10-10 [6] | 10.3 | 19.3 | 36.6 | 44.6 | 61.5 | 75.9 | 86.2 | 91.2 | 12.0 | 22.0 | 38.9 | 46.2 | 59.1 | 69.1 | 76.5 | 81.1 |
| LTD-10-25 [6] | 11.0 | 20.7 | 37.8 | 45.3 | 57.2 | 65.7 | 71.3 | 75.2 | 12.6 | 23.2 | 39.7 | 46.6 | 57.9 | 65.8 | 71.5 | 75.5 |
| Hisrep [21] | 11.3 | 20.7 | 35.7 | 42.0 | 51.7 | 58.6 | 63.4 | 67.2 | 12.6 | 23.1 | 39.0 | 45.4 | 56.0 | 63.6 | 69.7 | 73.7 |
| siMLPE(Ours) | 10.8 | 19.6 | 34.3 | 40.5 | 50.5 | 57.3 | 62.4 | 65.7 | 12.1 | 22.1 | 38.1 | 44.5 | 54.9 | 62.4 | 68.2 | 72.2 |

\mathcal{L}_v is a loss on velocity and aims at minimizing the difference between the velocity of the predicted motion $\mathbf{v}'_{T+1:T+N}$ and the ground truth one $\mathbf{v}_{T+1:T+N}$:

$$\mathcal{L}_v = \mathcal{L}_2(\mathbf{v}'_{T+1:T+N}, \mathbf{v}_{T+1:T+N}). \quad (5)$$

where $\mathbf{v}_{T+1:T+N} = [v_{T+1}^\top, \dots, v_{T+N}^\top]^\top \in \mathbf{R}^{N \times C}$, v_t represents the velocity at frame t and is calculated as $v_t = x_{t+1} - x_t$. We provide a full analysis on the loss terms in Section 4.5.

4 EXPERIMENTS

In this section, we present our experimental results. We first introduce datasets and evaluation metric in Section 4.1. Implementation details are provided in Section 4.2. We then present quantitative and qualitative results in Section 4.3. Finally, exhaustive analysis on the architecture, losses are detailed in Section 4.5.

4.1 Datasets and evaluation metric

Human3.6M [9] dataset. Human3.6M contains 7 actors performing 15 actions, 32 joints are labeled for each human. We use the same test protocols of [21], and use S5 as the test set, S11 as the validation set and the others as training set. Previous works use different testing sampling strategies, including 8 samples per action [6, 7], 256 samples per action [21] or all samples in the test set [24]. We take 256 samples per action for testing, and evaluate on 22 joints as in [6, 7, 21, 23].

AMASS [12] dataset. AMASS is a collection of multiple Mocap datasets [37–54] scandalized by SMPL [55] parameterization. We follow [21] to use BMLrub [41] as test set, and split the rest of AMASS [12] dataset into training and validation set. The model is tested on 18 joints for evaluation as in [21].

3DPW [13] dataset. 3DPW is a dataset including indoor and outdoor scenes. Each pose is represented by 26 joints. We follow [21] to evaluate on 3DPW [13] on 18 joints using the model trained on AMASS [12] to show the generalisation of our method.

Evaluation metric. We report Mean Per Joint Position Error (MPJPE) on 3D joint coordinates, which is the most widely used metric for evaluating 3D pose errors. This metric calculates the average l2-norm across different joints between the prediction and ground-truth. Similar with previous works [6, 21, 23, 24], we ignore the global rotation and translation of the poses and keep the sampling rate as 25 frame per second (FPS) for all datasets.

4.2 Implementation details

In practice, we set input length $T = 50$ and output length $N = 10$. During training, we take 50 frames as input and supervise only the first 10 frames of the output. During testing, we apply our model in an auto-regressive manner to generate motion for longer frames. The feature dimension $C = 3 \times K$, where K is the number of tested joints and varies across different datasets.

To train our network, we set batch size to 256 and use Adam [56] optimizer, the memory consumed by our net-

TABLE 3
Analysis of the number of MLP blocks on Human3.6M [9]. We report number of parameters in M as well as MPJPE error in *mm*.

| Nb. Blocks | # Param.(M) ↓ | MPJPE (mm) ↓ | | | | | | | |
|------------|---------------|--------------|-------------|-------------|-------------|-------------|-------------|--------------|--------------|
| | | 80 | 160 | 320 | 400 | 560 | 720 | 880 | 1000 |
| 1 | 0.012 | 12.7 | 28.5 | 59.7 | 72.1 | 93.6 | 107.0 | 116.8 | 123.6 |
| 2 | 0.014 | 10.9 | 24.9 | 52.3 | 64.0 | 83.2 | 97.3 | 108.4 | 115.4 |
| 6 | 0.025 | 10.2 | 23.1 | 48.8 | 60.1 | 79.0 | 93.3 | 105.1 | 112.6 |
| 12 | 0.041 | 9.9 | 22.4 | 47.2 | 58.3 | 77.1 | 91.5 | 103.3 | 110.9 |
| 24 | 0.073 | 9.7 | 22.0 | 46.8 | 57.7 | 76.4 | 90.8 | 102.6 | 110.3 |
| 48 (Ours) | 0.138 | 9.6 | 21.8 | 46.4 | 57.4 | 76.0 | 90.2 | 101.9 | 109.5 |
| 64 | 0.180 | 9.6 | 21.8 | 46.5 | 57.5 | 76.0 | 90.1 | 101.9 | 109.7 |
| 96 | 0.266 | 9.7 | 21.9 | 46.7 | 57.8 | 76.3 | 90.5 | 102.1 | 109.8 |

TABLE 4
Analysis of the MLP block on Human3.6M [9]. We report MPJPE error in *mm*.

| Transpose | Layer Norm | MPJPE (mm) ↓ | | | | | | | |
|-----------|------------|--------------|-------------|-------------|-------------|-------------|-------------|--------------|--------------|
| | | 80 | 160 | 320 | 400 | 560 | 720 | 880 | 1000 |
| | | 23.7 | 44.0 | 75.5 | 87.6 | 106.3 | 120.4 | 130.5 | 135.6 |
| | ✓ | 23.8 | 43.0 | 73.4 | 85.2 | 102.0 | 116.3 | 125.3 | 131.9 |
| ✓ | | 12.7 | 29.0 | 62.3 | 76.2 | 97.4 | 111.6 | 121.6 | 127.3 |
| ✓ | ✓ | 9.6 | 21.8 | 46.4 | 57.4 | 76.0 | 90.2 | 101.9 | 109.5 |

TABLE 5
Ablation of different losses on Human3.6M [9]. We report MPJPE error in *mm*.

| \mathcal{L}_{re} | \mathcal{L}_v | MPJPE (mm) ↓ | | | | | | | |
|--------------------|-----------------|--------------|-------------|-------------|-------------|-------------|-------------|--------------|--------------|
| | | 80 | 160 | 320 | 400 | 560 | 720 | 880 | 1000 |
| ✓ | | 9.6 | 21.8 | 46.5 | 57.5 | 76.7 | 91.5 | 103.5 | 111.3 |
| ✓ | ✓ | 9.6 | 21.9 | 46.5 | 57.5 | 75.8 | 90.1 | 101.8 | 109.5 |

work is about $2GB$ during the training. We repeat each experiment 5 times and take the average of the results. All our experiments are conducted using Pytorch [57] framework on a single NVIDIA RTX 2080Ti graphics card. We train our network on Human3.6M [9] dataset for 35k iterations, the learning rate starts from 0.0003 at the beginning and drops to 0.00001 after 30k steps. The training takes ~ 30 minutes. And we train our network on AMASS [12] dataset for 115k iterations, the learning rate starts from 0.0003 at the beginning and drops to 0.00001 after 100k steps. The entire training finishes in ~ 2 hours.

4.3 Comparison to state-of-the-art approaches

In this section, we compare our approach to existent state-of-the-art methods on different datasets. For each dataset, we report MPJPE in *mm* on different prediction time steps up to 1000ms.

Human3.6M [9] dataset. We compare our method with other state-of-the-art methods on Human3.6M dataset, as shown in Table 1. Our method outperforms all previous methods on every frame with much less number of parameters.

As explained in Section 4.1, different methods have taken different test sampling strategies, and we choose to test on 22 joints with 256 samples per action, following [21]. So to

make fair comparison, we evaluate all the methods using the same testing protocol. Previous works usually report short-term(0-500ms) and long-term(500-1000ms) predictions separately, and some works [23] report short-/long-term results using two different trained models. In our tables, all the results from 0 to 1000ms are generated by a single model, and for [23] we report results of their model which achieve the best performance on long term prediction.

In addition, we show two experimental results on the Human3.6m dataset in Table 1: ‘Last-frame’ takes the last input frame and repeat it N times as output, ‘One FC’ uses only one single fully connected layer trained on Human3.6m dataset. These two simple implementations could already achieve comparable results with early methods like [7].

AMASS [12] and 3DPW [13] dataset. In Table 2, we report performance of the model trained on AMASS dataset and tested on AMASS-BMLrub and 3DPW dataset, following the setting of [21]. Different from Human3.6m dataset where the training and testing data are same actions performed by different actors, the difference between training/testing data under this protocol is much bigger, which challenges the generalization of the method. We can see that our approach achieves competitive performances on short term prediction (80ms and 160ms) and perform consistently better on long-term prediction ($> 160ms$). More importantly, our model is much smaller and only contains $\sim 4\%$ parameters compared to Hisrep [21].

4.4 Qualitative result

Figure 3 shows some qualitative results of our methods comparing with other state-of-the-art methods, on Human3.6M dataset. The prediction of our methods is closer to the ground truth.

4.5 Ablation study

In this section, we ablate different components of our approach on Human3.6M dataset.

Number of blocks. We ablate the number of blocks n in Table 3. Our proposed architecture can already achieve reasonable performance using only 2 blocks, with parameter size of 0.014M. And the network achieves its best performance with 48 blocks.

Network Architecture. In Table 4, we ablate the components of our network. As shown in the table, the transpose operation and layer normalization [10] is of vital importance

to our network. Without the transpose operation, the network can only operate on spatial dimension of the motion sequence without merging any information across different frames, which leads to degraded results. This also reveals the fact that merging temporal information across different frames is the key of human motion prediction.

Loss. In Table 5 we ablate the importance of different loss terms used during training. As shown in the table, with the help of velocity loss \mathcal{L}_v , the network can achieve better performance on long term prediction while maintaining the same performance on short term.

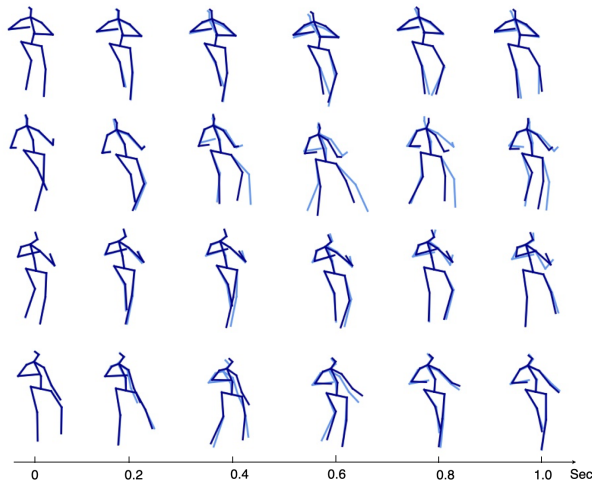


Fig. 3. Some qualitative results of our method siMLPE. The skeletons with light color are ground-truth, while those with dark color are predicted motions. Our prediction results are close to the ground-truth.

5 CONCLUSION

In this paper, we present siMLPE, a simple-yet-effective network for human motion prediction. Our network is composed of only fully connected layer, layer normalization and transpose operation. While using much less parameters, our network can achieve state-of-the-art performance on various benchmarks. We release our code and hope the simplicity of our method could help to community to rethink this task.

ACKNOWLEDGMENTS

This project has received funding from the CHIST-ERA IPALM project and was also supported by ANR-3IA MIAI (ANR-19-P3IA0003), ANR-JCJC ML3RI (ANR-19-CE33-0008-01), H2020 SPRING (funded by EC under GA #871245), by the Spanish government with the project MoHuCo PID2020-120049RB-I00 and by an Amazon Research Award.

REFERENCES

- [1] B. Paden, M. Čáp, S. Z. Yong, D. Yershov, and E. Frazzoli, “A survey of motion planning and control techniques for self-driving urban vehicles,” *Transactions on intelligent vehicles*, 2016. 1
- [2] H. Gong, J. Sim, M. Likhachev, and J. Shi, “Multi-hypothesis motion planning for visual object tracking,” in *ICCV*, 2011. 1
- [3] H. S. Koppula and A. Saxena, “Anticipating human activities for reactive robotic response.” in *IROS*, 2013. 1
- [4] M. Brand and A. Hertzmann, “Style machines,” in *Computer Graphics and Interactive Techniques*, 2000. 1
- [5] J. M. Wang, D. J. Fleet, and A. Hertzmann, “Gaussian process dynamical models for human motion,” *PAMI*, 2007. 1
- [6] W. Mao, M. Liu, M. Salzmann, and H. Li, “Learning trajectory dependencies for human motion prediction,” in *ICCV*, 2019. 1, 2, 3, 4
- [7] J. Martinez, M. J. Black, and J. Romero, “On human motion prediction using recurrent neural networks,” in *Proceedings of the IEEE Conference on Computer Vision and Pattern Recognition*, 2017, pp. 2891–2900. 1, 2, 3, 4, 5
- [8] E. Aksan, M. Kaufmann, P. Cao, and O. Hilliges, “A spatio-temporal transformer for 3d human motion prediction,” in *3DV*, 2021. 1, 2, 3
- [9] C. Ionescu, D. Papava, V. Olaru, and C. Sminchisescu, “Human3.6m: Large scale datasets and predictive methods for 3d human sensing in natural environments,” *PAMI*, 2013. 1, 2, 4, 5
- [10] J. L. Ba, J. R. Kiros, and G. E. Hinton, “Layer normalization,” *arXiv*, 2016. 2, 3, 5
- [11] V. Nair and G. E. Hinton, “Rectified linear units improve restricted boltzmann machines,” in *Icml*, 2010. 2
- [12] N. Mahmood, N. Ghorbani, N. F. Troje, G. Pons-Moll, and M. J. Black, “Amass: Archive of motion capture as surface shapes,” in *ICCV*, 2019. 2, 4, 5
- [13] T. von Marcard, R. Henschel, M. Black, B. Rosenhahn, and G. Pons-Moll, “Recovering accurate 3d human pose in the wild using imus and a moving camera,” in *European Conference on Computer Vision (ECCV)*, sep 2018. 2, 4, 5
- [14] A. M. Lehrmann, P. V. Gehler, and S. Nowozin, “Efficient nonlinear markov models for human motion,” in *CVPR*, 2014. 2
- [15] J. M. Wang, D. J. Fleet, and A. Hertzmann, “Gaussian process dynamical models,” in *NeurIPS*, 2005. 2
- [16] G. W. Taylor, G. E. Hinton, and S. T. Roweis, “Modeling human motion using binary latent variables,” in *NeurIPS*, 2007. 2
- [17] K. Fragkiadaki, S. Levine, P. Felsen, and J. Malik, “Recurrent network models for human dynamics,” in *ICCV*, 2015. 2
- [18] A. Jain, A. R. Zamir, S. Savarese, and A. Saxena, “Structural-rnn: Deep learning on spatio-temporal graphs,” in *CVPR*, 2016. 2
- [19] Z. Liu, S. Wu, S. Jin, Q. Liu, S. Lu, R. Zimmermann, and L. Cheng, “Towards natural and accurate future motion prediction of humans and animals,” in *Proceedings of the IEEE/CVF Conference on Computer Vision and Pattern*

- Recognition*, 2019, pp. 10 004–10 012. 2
- [20] H.-k. Chiu, E. Adeli, B. Wang, D.-A. Huang, and J. C. Niebles, “Action-agnostic human pose forecasting,” in *2019 IEEE Winter Conference on Applications of Computer Vision (WACV)*. IEEE, 2019, pp. 1423–1432. 2
- [21] W. Mao, M. Liu, and M. Salzmann, “History repeats itself: Human motion prediction via motion attention,” in *European Conference on Computer Vision*. Springer, 2020, pp. 474–489. 2, 3, 4, 5
- [22] W. Guo, X. BIE, X. Alameda-Pineda, and F. Moreno-Noguer, “Multi-person extreme motion prediction,” *CVPR*, 2022.
- [23] T. Ma, Y. Nie, C. Long, Q. Zhang, and G. Li, “Progressively generating better initial guesses towards next stages for high-quality human motion prediction,” in *CVPR*, 2022. 2, 3, 4, 5
- [24] L. Dang, Y. Nie, C. Long, Q. Zhang, and G. Li, “Msr-gcn: Multi-scale residual graph convolution networks for human motion prediction,” in *Proceedings of the IEEE/CVF International Conference on Computer Vision (ICCV)*, October 2021, pp. 11 467–11 476. 2, 4
- [25] M. Li, S. Chen, Y. Zhao, Y. Zhang, Y. Wang, and Q. Tian, “Dynamic multiscale graph neural networks for 3d skeleton based human motion prediction,” in *Proceedings of the IEEE/CVF Conference on Computer Vision and Pattern Recognition*, 2020, pp. 214–223.
- [26] M. Li, S. Chen, X. Chen, Y. Zhang, Y. Wang, and Q. Tian, “Symbiotic graph neural networks for 3d skeleton-based human action recognition and motion prediction,” *IEEE Transactions on Pattern Analysis and Machine Intelligence*, 2021. 2
- [27] J. Butepage, M. J. Black, D. Kragic, and H. Kjellstrom, “Deep representation learning for human motion prediction and classification,” in *Proceedings of the IEEE conference on computer vision and pattern recognition*, 2017, pp. 6158–6166. 2
- [28] J. Bütepage, H. Kjellström, and D. Kragic, “Anticipating many futures: Online human motion prediction and generation for human-robot interaction,” in *2018 IEEE international conference on robotics and automation (ICRA)*. IEEE, 2018, pp. 4563–4570. 2
- [29] A. Hernandez, J. Gall, and F. Moreno-Noguer, “Human motion prediction via spatio-temporal inpainting,” in *Proceedings of the IEEE/CVF International Conference on Computer Vision*, 2019, pp. 7134–7143. 2
- [30] C. Li, Z. Zhang, W. S. Lee, and G. H. Lee, “Convolutional sequence to sequence model for human dynamics,” in *Proceedings of the IEEE Conference on Computer Vision and Pattern Recognition*, 2018, pp. 5226–5234. 2, 4
- [31] L.-Y. Gui, Y.-X. Wang, X. Liang, and J. M. Moura, “Adversarial geometry-aware human motion prediction,” in *Proceedings of the European Conference on Computer Vision (ECCV)*, 2018, pp. 786–803. 2
- [32] A. Sperduti and A. Starita, “Supervised neural networks for the classification of structures,” *Transactions on Neural Networks*, 1997. 2
- [33] T. N. Kipf and M. Welling, “Semi-supervised classification with graph convolutional networks,” in *ICLR*, 2017. 2
- [34] T. Lebailly, S. Kiciroglu, M. Salzmann, P. Fua, and W. Wang, “Motion prediction using temporal inception module,” in *Proceedings of the Asian Conference on Computer Vision*, 2020. 2
- [35] A. Vaswani, N. Shazeer, N. Parmar, J. Uszkoreit, L. Jones, A. N. Gomez, L. Kaiser, and I. Polosukhin, “Attention is all you need,” in *Advances in Neural Information Processing Systems 30: Annual Conference on Neural Information Processing Systems 2017, December 4-9, 2017, Long Beach, CA, USA*, 2017. 3
- [36] Y. Cai, L. Huang, Y. Wang, T.-J. Cham, J. Cai, J. Yuan, J. Liu, X. Yang, Y. Zhu, X. Shen *et al.*, “Learning progressive joint propagation for human motion prediction,” in *European Conference on Computer Vision*. Springer, 2020, pp. 226–242. 3
- [37] Advanced Computing Center for the Arts and Design, “ACCAD MoCap Dataset.” [Online]. Available: <https://accad.osu.edu/research/motion-lab/mocap-system-and-data> 4
- [38] N. Mahmood, N. Ghorbani, N. F. Troje, G. Pons-Moll, and M. J. Black, “AMASS: Archive of motion capture as surface shapes,” in *ICCV*, 2019.
- [39] A. Aristidou, A. Shamir, and Y. Chrysanthou, “Digital dance ethnography: Organizing large dance collections,” *J. Comput. Cult. Herit.*, vol. 12, no. 4, Nov. 2019. [Online]. Available: <https://doi.org/10.1145/3344383>
- [40] B. M. Lab, “BMLhandball Motion Capture Database.” [Online]. Available: <https://www.biomotionlab.ca/>
- [41] N. F. Troje, “Decomposing biological motion: A framework for analysis and synthesis of human gait patterns,” *Journal of Vision*, vol. 2, no. 5, pp. 2–2, Sep. 2002. 4
- [42] Carnegie Mellon University, “CMU MoCap Dataset.” [Online]. Available: <http://mocap.cs.cmu.edu>
- [43] F. Bogo, J. Romero, G. Pons-Moll, and M. J. Black, “Dynamic FAUST: Registering human bodies in motion,” in *2017 IEEE Conference on Computer Vision and Pattern Recognition (CVPR)*, Jul. 2017, pp. 5573–5582.
- [44] E. J. C. Ltd., “Eyes Japan MoCap Dataset.” [Online]. Available: <http://mocapdata.com>
- [45] S. Ghorbani, K. Mahdaviani, A. Thaler, K. Kording, D. J. Cook, G. Blohm, and N. F. Troje, “MoVi: A large multipurpose motion and video dataset,” 2020.
- [46] A. Chatzitofis, L. Saroglou, P. Boutis, P. Drakoulis, N. Zioulis, S. Subramanyam, B. Kevelham, C. Charbonnier, P. Cesar, D. Zarpalas *et al.*, “Human4d: A human-centric multimodal dataset for motions and immersive media,” *IEEE Access*, vol. 8, pp. 176 241–176 262, 2020.
- [47] L. Sigal, A. Balan, and M. J. Black, “HumanEva: Synchronized video and motion capture dataset and baseline algorithm for evaluation of articulated human motion,” *International Journal of Computer Vision*, vol. 87, no. 4, pp. 4–27, Mar. 2010.
- [48] C. Mandery, Ö. Terlemez, M. Do, N. Vahrenkamp, and T. Asfour, “The kit whole-body human motion database,” in *ICAR*, 2015.
- [49] M. Loper, N. Mahmood, and M. J. Black, “MoSh: Motion and Shape Capture from Sparse Markers,” *ACM Trans. Graph.*, vol. 33, no. 6, Nov. 2014. [Online]. Available: <https://doi.org/10.1145/2661229.2661273>
- [50] M. Müller, T. Röder, M. Clausen, B. Eberhardt, B. Krüger, and A. Weber, “Documentation mocap

- database HDM05," Universität Bonn, Tech. Rep. CG-2007-2, Jun. 2007.
- [51] I. Akhter and M. J. Black, "Pose-conditioned joint angle limits for 3D human pose reconstruction," in *2015 IEEE Conference on Computer Vision and Pattern Recognition (CVPR)*, Jun. 2015, pp. 1446–1455.
- [52] S. F. University and N. U. of Singapore, "SFU Motion Capture Database." [Online]. Available: <http://mocap.cs.sfu.ca/>
- [53] L. Hoyet, K. Ryall, R. McDonnell, and C. O'Sullivan, "Sleight of hand: Perception of finger motion from reduced marker sets," in *Proceedings of the ACM SIGGRAPH Symposium on Interactive 3D Graphics and Games*, ser. I3D '12, New York, NY, USA, 2012, p. 79–86. [Online]. Available: <https://doi.org/10.1145/2159616.2159630>
- [54] M. Trumble, A. Gilbert, C. Malleson, A. Hilton, and J. Collomosse, "Total capture: 3d human pose estimation fusing video and inertial sensors," in *2017 British Machine Vision Conference (BMVC)*, 2017. 4
- [55] M. Loper, N. Mahmood, J. Romero, G. Pons-Moll, and M. J. Black, "Smpl: A skinned multi-person linear model," *ACM transactions on graphics (TOG)*, vol. 34, no. 6, pp. 1–16, 2015. 4
- [56] D. P. Kingma and J. Ba, "Adam: A method for stochastic optimization," *arXiv preprint arXiv:1412.6980*, 2014. 4
- [57] A. Paszke, S. Gross, F. Massa, A. Lerer, J. Bradbury, G. Chanan, T. Killeen, Z. Lin, N. Gimelshein, L. Antiga *et al.*, "Pytorch: An imperative style, high-performance deep learning library," *Advances in neural information processing systems*, vol. 32, 2019. 5